ULTRASOUND IMAGE SEGMENTATION USING LOCAL STATISTICS WITH AN ADAPTIVE SCALE SELECTION

Qing YANG and Djamal BOUKERROUI

Université de Technologie de Compiègne, Laboratoire Heudiasyc UMR-CNRS 7253
BP 20529 - 60205 Compiègne Cedex, France

ABSTRACT

We propose a region-based segmentation method based on local statistics. The adaptive spatial locality is defined using the Intersection of Confidence Intervals (ICI) approach. This pixel dependent local scale is estimated, conditionally on the current segmentation, in the sense of minimizing the mean-square error of a Local Polynomials Approximation (LPA). In other words, the scale is 'optimal' since it gives the best trade-off between the bias and the variance of the estimates. We provide a comparison with the single scale local region-based model. Results on simulated and real ultrasound images show that the proposed adaptive scale selection gives a robust solution to the attenuation problem.

Index Terms— local region statistics, Intersection of Confidence Intervals, ultrasound image segmentation.

1. INTRODUCTION

The use of statistical models in region-based image segmentation has a long tradition. Its introduction in active contour segmentation methods, mostly within the level set framework, has led to a considerable improvement in efficiency and robustness. For instance, the Chan-Vese (CV) model [1] and its variant [2] both consider image background and foreground as constant intensities represented by their mean values. The mean separation method [3] relies on the assumption that foreground and background should have maximally different intensities. These methods have many advantages and perform better than edge-based models in handling the noise and weak boundaries. However, they cannot deal with the intensity inhomogeneities, which is almost unavoidable.

Recently, some work has been carried out in utilizing local image statistics within the level set paradigm. For instance, a local binary fitting method has been proposed in [4]. A general framework for local region-based segmentation models has been presented in [5]. An interpretation of the piecewise smooth Mumford-Shah (MS) functional using local Gaussian models has been proposed in [6]. A local Gaussian distribution fitting energy is defined for the region-based active contour model in [7]. All of the above methods prove that the segmentation using local statistics has the ability to capture the boundaries of inhomogeneous objects.

Local region-based segmentation models, however, are found to be more sensitive to noise than global ones. Such models may also be more sensitive to initialization if the local scale is not appropriate. This brings out several problems that need to be addressed such as: Can global and local statistics be combined in one model? Is it possible to define a pixel dependent local scale from the estimation of image statistics? A first attempt within the level set framework has been proposed in [7]. Their approach is straightforward: it adds two energy functions of the same nature, where the model parameters are estimated globally in one and locally in the other. In fact, this is not the first time that global and local statistics are combined to solve a segmentation problem. To our knowledge, it is within the Bayesian framework that the first proposition has been introduced [8, 9].

This paper involves ideas described in [10] and applied to ultrasound (US) images. We propose a segmentation method based on local statistics with an adaptive local region, whose pixel dependent scale meets the counterbalance between the bias and the variance of estimations. Our method provides more desirable segmentation results compared to the single scale local region-based method [6].

2. LOCAL REGION-BASED SEGMENTATION

Recently, Brox and Cremers [6] have derived a statistical interpretation of the full MS functional [11] by relating it to recent works on local region statistics. They showed that the minimization of the piecewise smooth MS functional is equivalent to a first order approximation of a Bayesian a-posteriori maximization, basing on local region statistics. Thus this link is a consequence of the fact that local region models are not bounded by the strong assumption of identically distributed pixel intensities. Precisely, it is the approximation of the Bayesian setting with an additive noise of local Gaussian distribution, which can be expressed by the minimization of:

$$E(\phi) = \sum_r \int_{\Omega_r} \left[\frac{\big(I(\mathbf{x}) - \mu_r(\mathbf{x})\big)^2}{2\sigma_r^2(\mathbf{x})} + \frac{1}{2}\log\big(2\pi\sigma_r^2(\mathbf{x})\big) \right] d\mathbf{x} + \lambda \int_\Omega \delta(\phi(\mathbf{x}))|\nabla\phi(\mathbf{x})| d\mathbf{x} + \nu \int_\Omega H(\phi(\mathbf{x})) d\mathbf{x} \,, \quad (1)$$

where the subscript $r = \{i, o\}$ represent inside and outside of the segmentation contour C, and $\mathbf{x}$ is the spatial position in $\Omega \subset \mathbf{R}^2$. The image I is divided into foreground Ω_i and

background Ω_o by C. H is the Heaviside function of the level set function ϕ. The last two terms form the regularization term, whose contribution does not depend on image statistics. In Eq. (1), the local means and variances are functions of $\mathbf{x}$, and can be estimated using normalized convolutions:

$$\mu_r(\mathbf{x}) = \frac{\int_\Omega K_\hbar(\mathbf{x}-\zeta) H_r(\phi(\zeta))\, I(\zeta) d\zeta}{\int_\Omega K_\hbar(\mathbf{x}-\zeta) H_r(\phi(\zeta))\, d\zeta} \quad , \qquad (2)$$

$$\sigma_r^2(\mathbf{x}) = \frac{\int_\Omega K_\hbar(\mathbf{x}-\zeta) H_r(\phi(\zeta))\, (I(\zeta)-\mu_r(\mathbf{x}))^2\, d\zeta}{\int_\Omega K_\hbar(\mathbf{x}-\zeta) H_r(\phi(\zeta))\, d\zeta} \quad ,$$

where $H_i = H(\phi(\zeta))$, $H_o = 1 - H(\phi(\zeta))$. $K_\hbar(\cdot)$ can be any appropriate local kernel (often chosen to be the Gaussian kernel with a scaling parameter $\hbar$). The minimization of Eq. (1) is obtained when each point on C has moved, such that the local interior and local exterior of each point along C are best approximated by local means $\mu_r(\mathbf{x})$. A fast implementation using recursive filtering is given in [6] and references therein.

3. ADAPTIVE WINDOW SIZE BASED ON LPA-ICI

Suppose f is a function of the spatial position $\mathbf{x}$. We wish to reconstruct f using its noisy observations $I(\mathbf{x}_s) = f(\mathbf{x}_s) + \varepsilon_s$, $s = 1, \ldots, n$. The observations coordinates $\mathbf{x}_s$ are known, and ε_s are random errors with variance σ^2. Assume f can be approximated locally by members of a simple class of parametric functions. The LPA provides estimations in a point-wise manner, which finds the weighted least-square fitting in a sliding window. The estimate given by the LPA can be written as the kernel operator on the observations [12]:

$$\widehat{f}_h(\mathbf{x}) = \sum_s g_h(\mathbf{x}, \mathbf{x}_s) I(\mathbf{x}_s) \quad , \qquad (3)$$

where the kernel g_h is defined by the window w_h and the set of polynomials ψ_h. When the grid is assumed to be regular, the kernel $g_h(\mathbf{x}, \mathbf{x}_s)$ become shift-invariant on $\mathbf{x}$ and the solution is given by a convolution operation.

The ICI rule aims at searching for the largest local window size (minimizing local variances) where the LPA fits well to the observations (minimizing local bias). Let $\mathbf{h}$ be a set of the ordered scale values $\mathbf{h} = \{h_1 < h_2 < \ldots < h_J\}$. The estimates $\widehat{f}_h(\mathbf{x})$ are calculated for $h \in \mathbf{h}$ and compared. The ICI rule, which uses the estimates and their variances, identifies a scale closest to the ideal one. First a set of confidence intervals $Q(h)$ of the estimate is obtained [12]:

$$Q(h) = \left[\widehat{f}_h(\mathbf{x}) - \Gamma \cdot \sigma_{\widehat{f}_h}(\mathbf{x}, h),\ \ \widehat{f}_h(\mathbf{x}, h) + \Gamma \cdot \sigma_{\widehat{f}_h}(\mathbf{x}, h)\right]. \quad (4)$$

Here, $\sigma^2_{\widehat{f}_h}(\mathbf{x}, h) = \sigma^2 \sum_s g_h^2(\mathbf{x} - \mathbf{x}_s)$ is the standard deviation of the estimates, which can be estimated given the noise model and its variance σ^2. Eq. (4) is equivalent to: $\forall h_i \le h^*(\mathbf{x})$, $f_{h_i}(\mathbf{x}) \in Q(h_i)$ holds with probability p, related to the threshold Γ. Thus, for all $h_i < h^*$, the $Q(h_i)$ have a point in common, namely $f(\mathbf{x})$. If the ICI is empty, it indicates $h_i > h^*$. In this way, the ICI rule can test the existence of this common point and to obtain the adaptive scale. The ICI algorithm, which are point-wise repeated for each $\mathbf{x}$, is defined by the following steps:

1. Define a sequence of confidence intervals $Q_i = Q(h_i)$ with their lower bounds L_i and upper bounds U_i:
$$L_i = \widehat{f}_{h_i}(\mathbf{x}) - \Gamma \cdot \sigma_{\widehat{f}_{h_i}}(\mathbf{x}, h_i) \ ,$$
$$U_i = \widehat{f}_{h_i}(\mathbf{x}) + \Gamma \cdot \sigma_{\widehat{f}_{h_i}}(\mathbf{x}, h_i) \ .$$
2. For $i = 1, 2, \ldots, J-1$, let
$$\overline{L}_{i+1} = \max\{\overline{L}_i, L_{i+1}\}, \qquad \overline{L}_1 = L_1 \ ,$$
$$\underline{U}_{i+1} = \min\{\underline{U}_i, U_{i+1}\}, \qquad \overline{U}_1 = U_1 \ .$$
3. The ICI rule is finding the largest i, when $\overline{L}_i \le \underline{U}_i$, $i = 1, 2, \ldots, J$, is still satisfied.

4. PROPOSED METHOD

We propose applying the ICI approach to optimize the spatial adaptation for local region-based active contours. For each point, the ICI approach finds an optimal kernel size that permits the trade-off between the bias and the variance of estimates. This optimal local scale is then used for the estimation of the local means and variance of the segmentation model as given in Eq. (2). In this context, window size and scale are interchangeable concepts.

Suppose a noisy image I with intensity inhomogeneities in its foreground and background. We define an initial zero level set C, as the yellow contour shown in Fig. 1. Given a finite set of window sizes $\mathbf{h}$, we calculate the g_h for each element. Then utilize Eq. (3) to get the local estimations of the regions Ω_i and Ω_o respectively. It means that if a point $\mathbf{x}$ is inside of C, its approximation uses the local interior $\Omega_i^l(\mathbf{x}) = K_\hbar(\mathbf{x}) \bigcap \Omega_i$, and vice versa. As introduced in sec. 3, we can calculate the confidence intervals of this estimation, then apply the ICI algorithm for each point. After that, we obtain the optimal kernel size that well balances the bias-variance trade-off.

To find out the relation of these data adaptive scales with the position of the segmentation contour, we picked out several typical points for analysis. As we are only interested on a narrow band of C, within which we select 4 pairs of neighbors where one is in Ω_i (green '+') and the other is in Ω_o (red '$\circ$'). The corresponding estimated scales are also illustrated on the same figure with circles (Fig. 1, left). The leftmost pair P_4 lay around a region with very low contrast between Ω_i and Ω_o, where the local statistics are very similar. Also the contour near P_4 is the correct boundary, where the segmentation is locally achieved. In order to maintain this partition, we tend to consider more information, which is corresponding to

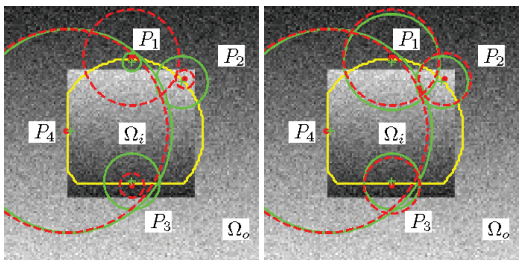


Fig. 1. Adaptive local kernel sizes. Left: obtained by LPA-ICI. Right: used in the segmentation.

the larger kernel size obtained by LPA-ICI algorithm. For the pair P_1 around the top of C, the inside one laying between C and the real boundary has small kernel size. This is expected, as in that position, larger windows will introduce greater estimation bias. Its symmetric point has, however, larger scale estimates, because in its neighboring region within Ω_o, the image is relatively homogenous. The pairs P_2 and P_3 have, however, larger window size inside and smaller one outside.

Therefore, if we directly use these kernel sizes in the segmentation algorithm, as C gets closer to the real boundary, the local regions of points between them are decreasing, and so will be the estimated local scale. This brings out the problem that the closer C is to the correct segmentation, the slower the evolution speed is. Analyzing case P_1 (P_2), the scale inside (outside) has to be at least as big as the outside (inside) in order to increase the force driving the segmentation process. To accelerate the evolution, we run a max filter of a small size 3×3, on the estimated local scales, so that near C, the used scales have similar values (Fig. 1, right). This filtering operation is necessary only when the algorithm is in progress. Indeed, the estimated scales are very appropriate as it can be seen on the correct segmentation P_4.

Our algorithm is organized as follows:

1. Initialization: Given an image I, an initial segmentation C or ϕ, a finite set $\mathbf{h}$ and a vector of polynomials ψ. For each $h \in \mathbf{h}$ calculate the LPA kernel g_h.
2. Optimal spatial kernel size estimation–LPA-ICI: Estimate respectively the image inside and outside of C with g_h. Apply the ICI rule in order to get $\widehat{h}$.
3. Local region-based segmentation: Use the local statistics within $\widehat{h}$ for full MS segmentation [6].
4. Repeat steps 2 and 3 until convergence.

5. EXPERIMENT AND DISCUSSION

This section demonstrates the performance of the proposed adaptive segmentation algorithm and compare it with the single local scale method [6], which explains the importance of the adaptive selection of local scales in order to achieve acceptable results. We denote by $\widehat{h}$ the half window size and by $\hbar$ the kernel standard deviation.

Fig. 2 shows a desirable segmentation result of the image in Fig. 1 with the proposed method. For a further analysis, plots of the estimated local window sizes $\widehat{h}$ along the final contour, for the inside and the outside regions are also shown. These plots follow a pixel clockwise parametrization of the curve starting from the top right corner. Notice for example that the estimated scales in Ω_i are smaller than the outside region. This can be explained by the fact that the inhomogeneity in Ω_i is stronger than that in Ω_o. This difference of scales, between the inside and the outside, is important for the forces in competition around low contrasted boundaries.

Then, we chose to test the proposed method on US B-mode image, which are known to have low signal-to-noise ratio, low contrast, and high amounts of speckle. Consequently,

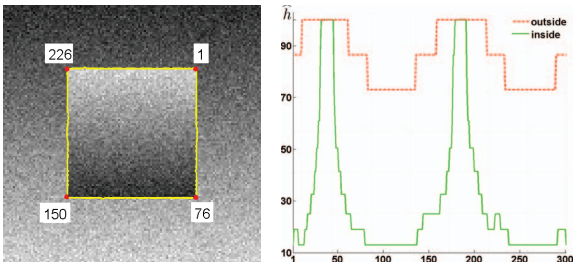


Fig. 2. Left: segmentation result of the proposed method, the initial curve is shown in Fig. 1. Right: the estimated optimal spatial kernel sizes, clockwise along C, for the Ω_i and Ω_o.

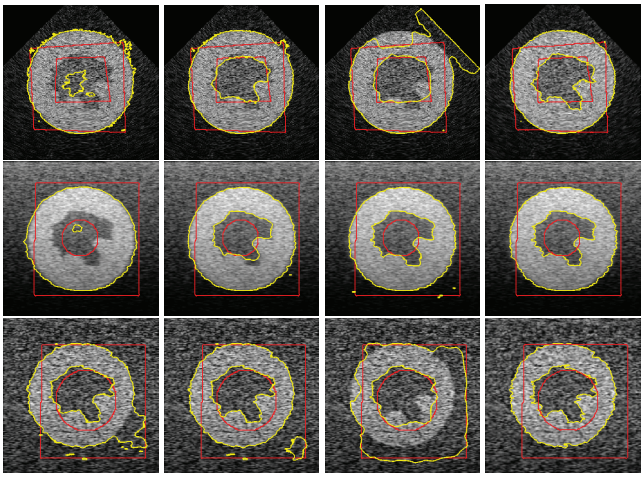


Fig. 3. Segmentation of simulated US images. From left to right: local MS with the $\hbar = 70, 40, 10$; the proposed method. From top to bottom: 'PH1_45dB', 'PH2_ATT2_65dB' and 'PH3_35dB' with 3 different initializations.

US image segmentation is strongly influenced by the quality of data [13]. Our main objective, is not to solve this difficult problem, but to show that adaptive scale selection gives an acceptable solution to the attenuation problem. Therefore, we chose to demonstrate the proposed approach on realistic US simulations. We have used the US simulation program Field-II [14] to synthesize data with known ground truth. For example, the first phantom (PH1) of size 100 mm cube was placed at 10 mm depth from the transducer surface, and was scanned with a 7 MHz 128 elements phased array transducer. A single transmit focus at 60 mm from the transducer was used, and focusing during reception is at 10 to 150 mm in 1 mm increments. The images consist of 128 lines with 0:7 degrees between lines. Hanning apodization in transmit and receive was used in all experiments. Three levels of tissue attenuations were simulated for each phantom. We also used different dB ranges for the envelope log compression to simulate different image contrasts.

Fig. 3 shows some segmentation results obtained by the local MS model for 3 scales and by the proposed adaptive scale algorithm. Notice the influence of the choice of size of the windows for the local method with single scale. Our proposed scale selection gives better results.

In order to further study the influence of the kernel size

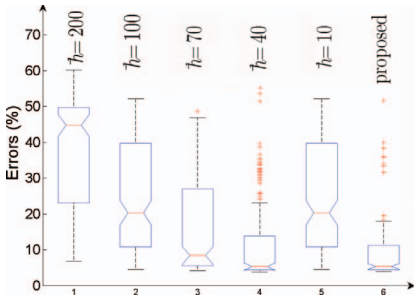


Fig. 4. Error bars of DSC

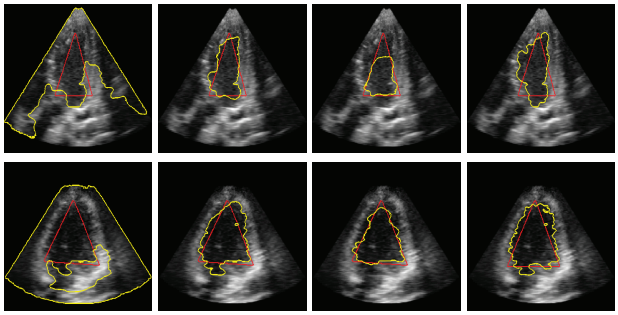


Fig. 5. Segmentation of US images. Top line from left to right: local MS method with $\hbar = 6, 4, 2$ and the proposed method; bottom one: local MS method with $\hbar = 9, 8, 3$ and the proposed method.

in single scale local region-based method, Fig. 4 shows the quantitative comparison between the proposed approach to the single scale LMS method. The error bar shows statistics of the Dice similarity Coefficient ($1 - \text{DSC} = 1 - 2\frac{|S \bigcap S_{ideal}|}{|S|+|S_{ideal}|}$) of 60 images of the simulated 3 phantoms with 3 different initializations (overall $60 \times 3 = 180$ images). The DSC statistics shows clearly that, when $\hbar = 200, 100$, the local MS model is equivalent to the global Gaussian model in [2]. For the scale $\hbar = 70, 10$, as the images shown in Fig. 3, the segmentations have high variability of errors. For these test images, the local MS method using $\hbar = 40$ provides a significant improvement with respect to the other 4 kernel sizes, however, its DSC errors still have larger variance and more outliers than the proposed adaptive one. This is expected since the appropriate scale should depend on the specific cases, such as the position of the initial C, the noise level and the size of the target. Therefore, the proposed adaptive segmentation algorithm has an increase of robustness to initialization and to attenuation.

Finally, we show some preliminary results on real US images in Fig. 5. The local MS method, using a fixed scales statistics, has varying results. An appropriate scale is necessary in the application of local region-based segmentation, while the proposed method need not.

6. CONCLUSIONS

In this paper, we presented a local region-based segmentation method with adaptive scale selection within the level set framework. The ICI rule is used to derive the optimal scales for interior and exterior of the current segmentation. We showed the results of the proposed method with comparisons to the single scale local MS model, and the statistics of the segmentations for 60 simulated US images with 3 different initializations. All of these illustrate the improvement on the state of the art of segmentation methods. Although our experiments on the real US images are limited, it suggest the proposed method has potential application. The continued development of the proposed method, with more experiments, should be researched in the foreseeable future.

Acknowledgements: The authors would like to thank Professor Alison Noble form the BioMedIA Laboratory, University of Oxford, for providing us the real US data. Financial supports of this research from the Chinese Scholarship Council and the Laboratoire Heudiasyc are greatly appreciated.

7. REFERENCES

[1] T. F. Chan and L. A. Vese, "Active contours without edges," *IEEE Trans. Image Process.*, vol. 10, no. 2, pp. 266–277, 2001.

[2] M. Rousson, T. Brox, and R. Deriche, "Active unsupervised texture segmentation on a diffusion based feature space," Tech. Rep. 4695, INRIA, 2003.

[3] A. Yezzi, A. Tsai, and A. Willsky, "A fully global approach to image segmentation via coupled curve evolution equations," *J. Visual Communication Image Representation*, vol. 13, no. 1-2, pp. 195–216, 2002.

[4] C. Li, C. Kao, J. C. Gore, and Z. Ding, "Minimization of region-scalable fitting energy for image segmentation," *IEEE Trans. Image Process.*, vol. 17, no. 10, pp. 1940–1949, 2008.

[5] S. Lankton and A. Tannenbaum, "Localizing region-based active contours," *IEEE Trans. Image Process.*, vol. 17, no. 11, pp. 2029–2039, 2008.

[6] T. Brox and D. Cremers, "On local region models and a statistical interpretation of the piecewise smooth Mumford-Shah functional," *Int. J. Comput. Vis.*, vol. 84, no. 2, pp. 184–193, 2009.

[7] L. Wang, C. Li, Q. Sun, D. Xia, and C. Kao, "Active contours driven by local and global intensity fitting energy with application to brain MR image segmentation," *Comput. Med. Imaging Graph.*, vol. 33, no. 7, pp. 520–531, 2009.

[8] D. Boukerroui, O. Basset, A. Baskurt, and A. Noble, "Segmentation of echocardiographic data. Multiresolution 2D and 3D algorithm based on gray level statistics," in *MICCAI*, 1999.

[9] D. Boukerroui, A. Baskurt, A. Noble, and O. Basset, "Segmentation of ultrasound images–multiresolution 2D and 3D algorithm based on global and local statistics," *Pattern Recognit. Lett.*, vol. 24, pp. 779–790, 2003.

[10] Q. Yang and D. Boukerroui, "Optimal spatial adaptation for local region-based active contours: An intersection of confidence intervals approach," in *VISIGRAPP*, 2011, pp. 87–93.

[11] D. Mumford and J. Shan, "Optimal approximations by piecewise smooth functions and associated variational problems," *Communications on Pure and Applied Mathematics*, vol. 42, pp. 577–685, 1989.

[12] V. Katkovnik, K. Egiazarian, and J. Astola, "Adaptive window size image de-noising based on intersection of confidence intervals (ICI) rule," *J. Math. Imag. Vis.*, vol. 16, no. 3, pp. 223–235, 2002.

[13] A. Noble and D. Boukerroui, "Ultrasound image segmentation: A survey," *IEEE Trans. Med. Imaging*, vol. 25, no. 8, pp. 987–1010, 2006.

[14] J. A. Jensen, "Field: A program for simulating ultrasound systems," in *10th Nordic-Baltic Conf. on Biomedical Imag.*, 1996, vol. 34, pp. 351–353.